MULTIOBJECTIVE OPTIMIZATION FOR THE ADVANCED PHOTOINJECTOR EXPERIMENT (APEX)*

C.F. Papadopoulos†, J. Corlett, D. Filippeto, J. Qiang,
F. Sannibale, J. Staples, M. Venturini, M. Zolotorev
LBNL, Berkeley, CA, USA

Abstract

The Advanced Photoinjector Experiment (APEX) is part of the Next Generation Light Source (NGLS), a proposed soft x-ray FEL concept being studied at LBNL. The requirements for the beam delivered to the FELs pose restrictions on the beam parameters at the injector. In addition, different modes of operation of the machine may pose different requirements on the beam.

In order to optimize the performance of the injector, a genetic multiobjective algorithm has been used. A genetic algorithm is used because of the inherent complexity of the beam dynamics at the energy range in question (0-30 MeV) and the large number of parameters available for optimization. On the other hand, the multiplicity of requirements on the beam, which include beam emittance, beam pulse length, energy chirp, as well as pulse shape and peak current, leads to a multiobjective approach for the optimization technique.

In this paper, we present the status of the optimization simulations, using the ASTRA particle-in-cell code. A number of different solutions for a range of bunch charges are presented and the resulting transport solutions are compared to each other and the requirements of the downstream sections of the accelerator.

DESIGN OF THE APEX PHOTOINJECTOR

The APEX photoinjector is in the active design and construction stage and will serve as a platform for proving the performance of the VHF electron gun designed in Lawrence Berkeley National Lab.

The components included in the injector transport line serve a number of functions, most importantly to provide transverse and longitudinal control of the electron beam, as well as to accelerate it. Since the beam energy at the exit of the gun is 750 keV, space charge phenomena such as emittance growth and longitudinal or transverse tails (halo) can be significant.

Additionally, the standard emittance compensation procedure [1] is needed to remove the correlated component of the transverse emittance and thus reduce the emittance, in accordance with the requirements of the FEL undulators downstream.

* This work was supported by the Director of the Office of Science of the US Department of Energy under Contract no. DEAC02-05CH11231
† cpapadopoulos@lbl.gov

In Fig. 1 we show a conceptual schematic of the injector, based on standard components. The frequency of the VHF Gun is 187 MHz, and the beam energy at its exit is 750 keV. A more detailed discussion of the VHF gun is provided in [2]. The single cell buncher cavity is based on designs from Cornell University [3] and it operates at 1.3 GHz, with a maximum accelerating voltage of 200 keV. The accelerating RF cavities are 7 cell structures and also have an operating frequency of 1.3 GHz with an accelerating field up to 10 MV/m. They are based on designs from Argonne National Lab [4].

Based on the above values, the beam energy at the end of the injector can be up to 30 MeV, but is typically in the 15-20 MeV range, since the beam is injected off-crest to achieve longitudinal compression.

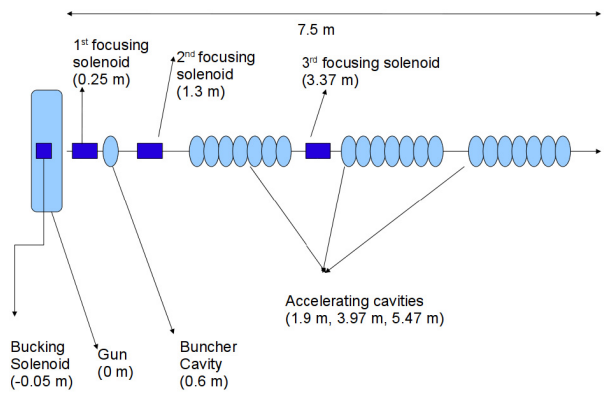

Figure 1: Conceptual design of the APEX photoinjector. The 3 solenoids are used for emittance compensation as well as transverse focusing. Longitudinal compression is achieved by using the buncher cavity as well as by dephasing the first two accelerating sections.

The exact values of the magnitude and phases of the RF fields, as well as the initial spot size and pulse length of the laser that creates the electron beam at the photocathode, are determined by the optimization process. Since the simulation code used (see below) includes space charge effects, and the fields of the transport line components are realistic, we expect our model to be a good approximation of the real beam.

A number of different cathodes will be tested in the APEX facility, but the operational focus will be on cesium telluride based photo-emitters. For the latter, there exist measured values for the thermal emittance [5], which give a value for the transverse velocity spread $\sqrt{< x'^2 >} \sim 1$ mrad, and this value is used as an initial condition for our

simulations.

The emittance evolution for a typical solution for a charge of 300 pC is shown in Fig. 2

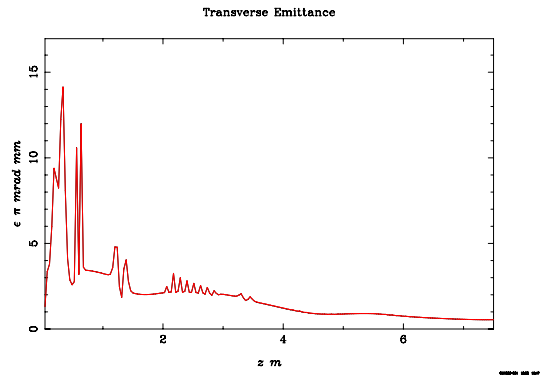

Figure 2: Evolution of the transverse emittance ϵ_{nx} along the injector for Q=300 pC.

As seen from Fig. 2, the emittance compensation process is not simple in the case of multiple solenoids and accelerating sections. Nonetheless, using the genetic optimizer we are still able to find a solution within the operational constraints of the different components and initial conditions.

The 3-stage longitudinal compression for the same solution is shown in Fig. 3

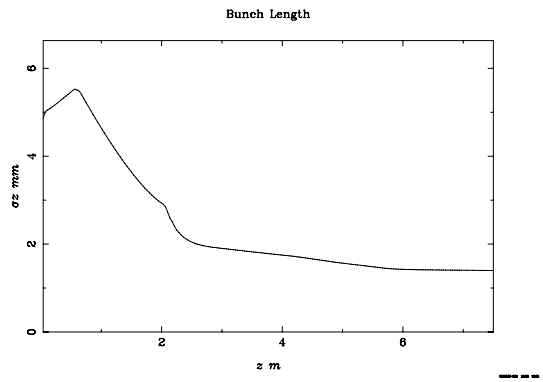

Figure 3: Evolution of the bunch length along the injector for Q=300 pC. Note the 3-stage compression.

Six Dimensional Brightness

Another important quantity for beam dynamics is the six dimensional brightness, which is a figure of merit for the compactness of the full, six dimensional phase space of the electron beam.

In the following, we define this as:

$$B_{6D} = \frac{Q}{\epsilon_{nx}\epsilon_{ny}\epsilon_{nz}} \qquad (1)$$

where Q is the total bunch charge, the normalized transverse emittance is given by $\epsilon_{nx} = \beta\gamma\sqrt{< x^2 >< x'^2 > - < xx' >^2}$ and similarly for y and the normalized longitudinal emittance is

$$\epsilon_{nz} = \frac{1}{mc}\sqrt{< z^2 >< p_z^2 > - < zp_z >^2} \qquad (2)$$

One of the important properties of B_{6D} is that it is conserved in the presence of linear forces, even in the case of coupling between longitudinal and transverse dynamics.

Single and Multiobjective Optimization

The use of multiobjective optimization techniques for the design of photoinjectors was originated by Bazarov and Sinclair [6] and these techniques have become a standard tool for optimizing the design of multicomponent transport lines.

In this case, the optimization algorithm produces a population of solutions, each with a different value for the two or more objectives to be minimized. Focusing on the simplest case of two objectives, the final result is a population of solutions along a 1D curve in the 2D plane of objectives.

In our case, we have made extensive use of the NSGA-II algorithm [7], a widely used genetic algorithm for multiobjective optimization. Additionally, the widely used Particle-In-Cell (PIC) code ASTRA [8] was applied for simulating the beam transport.

The choice of objectives to be minimized depends on the final requirements at the undulators of the FEL. Since even analytical models of the FEL performance [9] include a significant number of input parameters, a choice must be made for the objectives of the optimization.

Two of the most important factors are the transverse emittance and the length of the electron beam. Due to the cylindrical symmetry of the system, as well as the fact that the beam is being accelerated across the transport line, we focus on the normalized x-component of the emittance. Hence, we optimize for ϵ_{nx} and σ_z at the end of the injector.

Another mode of operation of the genetic optimizer is the more widely known single objective optimization. In this case, the six dimensional brightness discussed previously is a plausible measure of the beam quality. The optimization algorithm will produce a single solution that has the maximum B_{6D}, instead of a range of solutions along an optimal curve.

One reason for choosing B_{6D} as an optimization parameter is the fact that it is conserved under linear forces, and hence is a natural first choice for a "figure of merit" quantity in the case of coupling between transverse and longitudinal dynamics. Furthermore, the FEL performance will depend on the compactness of phase space, particularly for low bunch charges. In the case of higher charge and longer pulses, operational experience from the LCLS [10] shows that the energy spread needs to be degraded by using a laser heater, in order to avoid microbunching. Hence, for high charge, the optimization has to be applied to transverse emittance and peak current instead of B_{6D}.

SCALINGS WITH CHARGE

Motivation

The design studies for NGLS require different types of beamlines, and each of those translate to different requirements on the characteristics of the beam coming out of the injector, especially regarding the bunch charge. Hence, we need to understand the scalings of the relevant quantities such as emittance with charge.

Following the scalings from [11] and [12], we expect that for pulse lengths much shorter than the RF period of the cavities and the gun, the transverse and longitudinal size should scale as $\sigma_z \sim Q^{1/3}$ and $\sigma_x \sim Q^{1/3}$. This scaling implies that the charge volume density is held constant.

Additionally, in the case of emittance growth solely due to space charge, the transverse and longitudinal emittances are expected to scale as $\epsilon_{nx} \sim \sigma_x^2$ and $\epsilon_{nz} \sim \sigma_z^2$ respectively [12]. This leads to a scaling of $\epsilon_{nx} \sim Q^{2/3}$ and $\epsilon_{nz} \sim Q^{2/3}$ for the projected emittances and $B_{6D} \sim Q^{-1}$ for the six dimensional brightness.

These scalings will of course change if quantities other than the beam density are kept constant as the bunch charge is varied.

Simulation Results

As noted previously, we use the ASTRA code to model the photoinjector. Additionally, all of the input parameters were kept within realistic limits, and we have relied on proven technologies for all the transport line elements.

In Fig. 4 we plot the results from the multiobjective optimizer for different bunch charges.

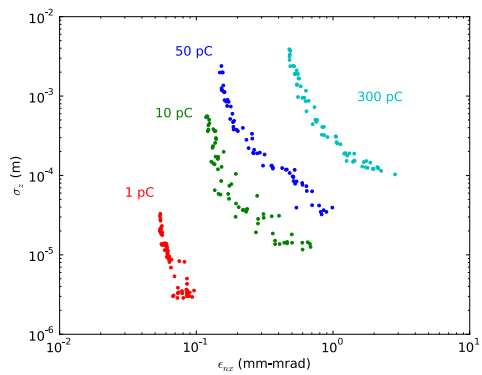

Figure 4: Optimum curve for different bunch charge values. The solutions present a range of choices for pulse length and transverse emittance.

As seen in Fig. 4, the bunch charge affects the range of values for bunch length and emittance.

The comparison of solutions for different charges for the single- and multi-objective cases is shown in Figs. 5 and 6.

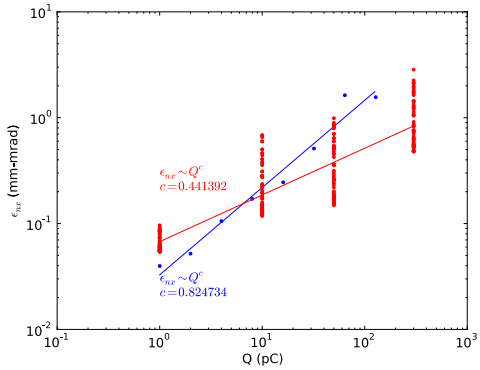

Figure 5: Scaling of ϵ_{nx} with charge for single objective (blue) and two objective (red) optimization.

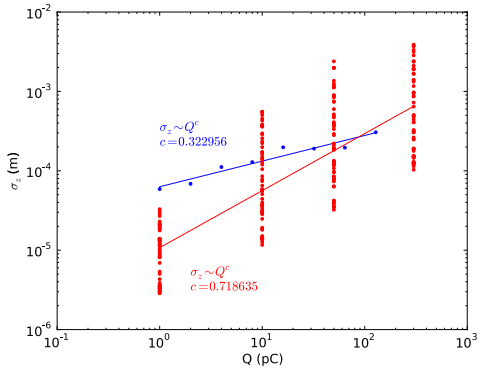

Figure 6: Scaling of σ_z with charge for single objective (blue) and two objective (red) optimization.

Discussion

We see that optimizing for a single objective and optimizing for 2 objectives yield similar, but not identical results. The scaling of ϵ_{nx} and σ_z with charge for both cases does not follow the expected result, but the trend holds. Especially for the case of two-objective optimization, the spread of the solutions means that the injector is operated in different regimes, such as high- and low-compression.

The main advantage of the multiobjective case is that a population of solutions is produced, instead of single point. Effectively, this means that the "tweaking" that is usually needed for beam operations is itself modeled. Thus, the limits of what can be achieved are also estimated.

In the case of picking an operating charge, we see that for the same value of Q, a wide range of pulse lengths and transverse emittances are achievable. The scaling laws derived may serve as a guide for designing the transport line, but due to the multiparametric nature of the problem, accurate simulations are needed for realistic designs.

REQUIREMENTS FOR THE NGLS FEL

As mentioned before, the simulations presented in the present paper do not include acceleration to the GeV range,

as required for NGLS. Furthermore, additional compression is required to reach the range for the peak bunch current at the undulators. Although accurate simulations of the accelerating linac are needed to fully model the transport from the injector to the undulators, the expectation is that the transverse emittance should not be significantly degraded after the injector.

Nominal values for peak current, emittance and bunch length at the undulators are given in Table 1 Assuming a

Table 1: Nominal Beam Requirements for good FEL Performance for Different Beamline Types

	Charge (pC)	
	10	300
Emittance (mm-mrad)	0.1–0.2	0.8
Peak Current (A)	300	500
Bunch Length (fs)	Single spike mode	300

compression factor of 15-20, the parameters of Table 1 can be scaled to the injector exit to 15-20 A peak current for the 10 pC case and 25-35 A peak current over 4.5-6 ps for the 300 pC case.

In Fig. 7 we plot one possible solution for the 300 pC, while in Fig. 8 we show a solution for 10 pC that satisfies the constraints.

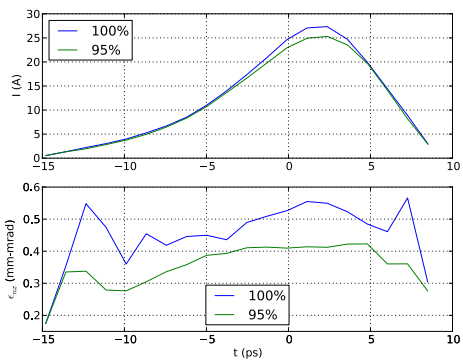

Figure 7: Slice current (upper) and slice ϵ_{nx} (lower) for Q=300 pC at the end of the injector. Note the difference between 100% and 95% emittance.

CONCLUSION

In this paper we show that the design parameters proposed for the NGLS are feasible for a range of bunch charges. The solutions found provide guidance for the design and operation of the APEX photoinjector facility.

ACKNOWLEDGEMENTS

This work was supported by the Director of the Office of Science of the US Department of Energy under Contract no. DEAC02-05CH11231. We would like to thank Claudio Pellegrini, Jonathan Wurtele and Gregory Penn for their input regarding the FEL simulations.

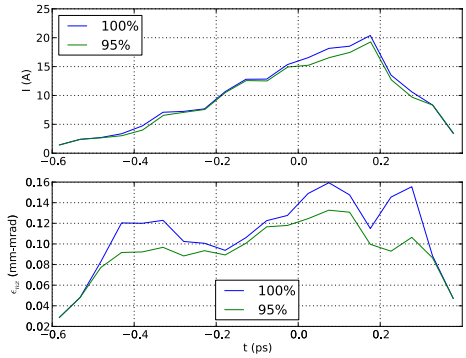

Figure 8: Slice current (upper) and slice ϵ_{nx} (lower) for Q=10 pC at the end of the injector.

REFERENCES

[1] L. Serafini et al. Envelope analysis of intense relativistic quasilaminar beams in rf photoinjectors: mA theory of emittance compensation. *Physical Review E*, 55(6):7565–7590, 1997.

[2] F. Sannibale et al. Status of the LBNL Normal-conducting CW VHF Electron photo-gun. In *Proceedings of the Free Electron Laser Conference*, 2010.

[3] V. Veshcherevich et al. Buncher Cavity for ERL. *Proc. of PAC03*, pages 1198–1200.

[4] JG Power et al. Upgrade of the drive linac for the AWAs facility dielectric two-beam accelerator. In *Proceedings of IPAC 2010*.

[5] V. Miltchev et al. Measurements of thermal emittance for cesium telluride photocathodes at PITZ. In *Proceedings of the Free Electron Laser Conference*, 2005.

[6] Ivan V. Bazarov and Charles K. Sinclair. Multivariate optimization of a high brightness dc gun photoinjector. *Physical Review Special Topics - Accelerators and Beams*, 8(3):034202+, Mar 2005.

[7] K. Deb. *Multi-objective optimization using evolutionary algorithms*. Wiley, 2001.

[8] K. Flöttmann. ASTRA: A space charge tracking algorithm. *user's manual available at http://www. desy. de/˜ mpyflo/Astra_dokumentation*.

[9] M. Xie. Exact and variational solutions of 3D eigenmodes in high gain FELs* 1. *NIMA: Accelerators, Spectrometers, Detectors and Associated Equipment*, 445(1-3):59–66, 2000.

[10] P. Emma et al. First lasing and operation of an ångstrom-wavelength free-electron laser. *Nature Photonics*, advance online publication, August 2010.

[11] K. Kim. Rf and space-charge effects in laser-driven rf electron guns. *NIMA: Accelerators, Spectrometers, Detectors and Associated Equipment*, 275(2):201–218, February 1989.

[12] J. Rosenzweig et al. Charge and wavelength scaling of RF photoinjector designs. In *AIP Conference Proceedings*, pages 724–737. IOP INSTITUTE OF PHYSICS PUBLISHING LTD, 1995.